High Frequency Transducer Characterization with a Sagnac Interferometer

James L. Bonnett and T. Buma
Department of Electrical and Computer Engineering
University of Delaware
Newark, DE 19716
buma@ece.udel.edu

Abstract— Optical techniques achieve extremely fine spatial resolution and broad detection bandwidth for high frequency transducer characterization. We demonstrate that a Sagnac interferometer can map the pressure field from a spherically focused high frequency lithium niobate transducer. The common path nature of the Sagnac interferometer provides immunity to perturbations, a significant advantage for practical applications. The optical spot size on the sensing surface is measured to be 8 μm, and the photodetector bandwidth is 150 MHz. Single-shot waveforms have a signal-to-noise ratio of 23 dB. The measured -3 dB transmit beam width of the transducer is 40 μm along both x and y axes. The sidelobe level is -21 dB. The Sagnac and pulse echo data have peak frequencies of 80 MHz and 95 MHz, respectively. The corresponding -6 dB bandwidths are 75 MHz and 70 MHz, respectively. The slight difference is expected since the pulse echo spectrum is shaped by the two-way response of the transducer. Based on a comparison to a calibrated PVDF hydrophone at lower frequencies, the single-shot noise equivalent pressure of the Sagnac interferometer is 38 kPa. These results demonstrate the potential of the Sagnac interferometer for high frequency transducer characterization.

Keywords-Sagnac; interferometer; high frequency; ultrasound biomicroscopy; transducer characterization

I. INTRODUCTION

Ultrasound biomicroscopy employs frequencies higher than 50 MHz to achieve fine spatial resolution. Progress in high frequency transducer fabrication offers the potential of miniaturized, minimally invasive ultrasound imaging systems with unprecedented resolution. Accurately measuring the transmitted ultrasound is clearly an important procedure in developing high frequency transducers. Unfortunately, such basic information is difficult to obtain due to the lack of suitable hydrophones operating at frequencies higher than 50 MHz. Optical detection of ultrasound provides both fine spatial resolution and large bandwidth. Light can be easily focused down to spot sizes less than 10 μm, which is less than an acoustic wavelength in water for 100 MHz ultrasound. Photodetector bandwidths over 1 GHz are readily available, providing more than sufficient bandwidth for measuring high frequency ultrasound transducers.

Optical detection of ultrasound is typically performed with an interferometer. The classic example is a Michelson interferometer, where incident ultrasound modulates one mirror of the interferometer [1]. Traditionally, optical detection of ultrasound suffers from low sensitivity. However, sensitivities comparable to piezoelectric detection have been demonstrated with optical etalon sensors [2-4]. We are exploring a different type of interferometer, called a Sagnac interferometer, for high frequency ultrasound detection. The Sagnac interferometer has been used for detecting lower frequency ultrasound (i.e. 1 – 10 MHz), particularly for applications in nondestructive evaluation [5-7]. This paper investigates the performance of the Sagnac interferometer for detecting ultrasound beyond 100 MHz.

II. METHODS

A. Sagnac interferometer

The Sagnac interferometer can be understood by considering an optical pulse incident on a set of optics, to be described in more detail later. As shown in Fig. 1(a), the pulse is split in two, where the leading pulse and lagging pulse are separated by a fixed time delay τ. Therefore, the two pulses probe the vibrating surface displacement d(t) at slightly different times. The reflected pulses are sent back through the optical system, which removes the time delay between the two pulses (Fig. 1(b)). The overlapping pulses interfere to yield a photodetector signal proportional to $d(t) - d(t-\tau)$. Therefore, the Sagnac interferometer probes surface velocity. The Sagnac interferometer is inherently immune to perturbations due to its "common path" nature, where the two interfering pulses travel the same optical path. This is a significant practical advantage over many other types of interferometers (i.e. Michelson) requiring active stabilization. Only passive components (e.g. waveplates and polarizers) are necessary for proper operation.

The details of the optical system are shown in Fig. 2. Instead of using a pulsed source, the Sagnac interferometer is operated with a superluminescent diode (SLD). An SLD is essentially a continuous output, high power light emitting diode with high spatial coherence. The peak wavelength is 1290 nm

This work is supported by NIH R21 grant EB006750.

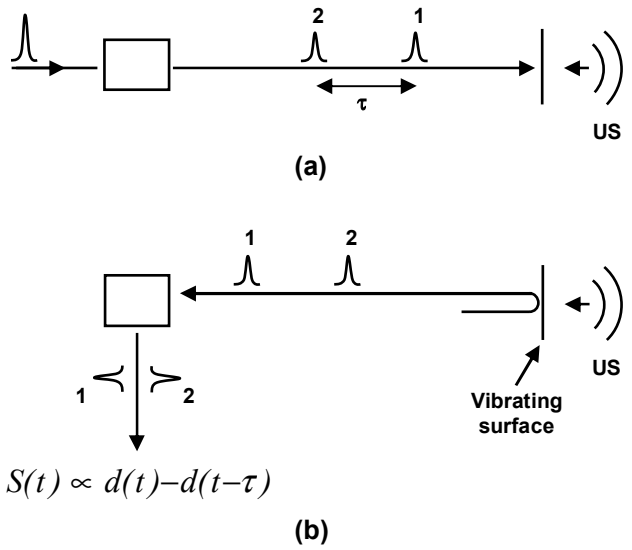

Figure 1. (a) The incident pulse is split into a leading pulse "1" and lagging pulse "2" separated by a time delay τ. The two pulses probe a reflective surface modulated by ultrasound (US). (b) The time delay is removed from the return pulses, which interfere to produce a signal S(t).

with a 45 nm bandwidth. The broad bandwidth produces a short coherence length, which is the effective "pulse" for the Sagnac interferometer. The short coherence length of this source suppresses optical beat noise in the interferometer [8], which is built from bulk optics. The SLD output is polarized at 45 degrees and sent towards two polarizing beamsplitters (PBSs). The horizontally polarized light passes through the PBS pair and takes the "short" path to the transducer. The vertically polarized light is reflected by the PBS pair and takes the "long" path. Therefore, the horizontal and vertical polarizations correspond to the leading and lagging pulses, respectively. The path length difference is 0.6 m, corresponding to a time delay of 2 ns. The combination of the quarter wave plate (QWP) and reflection off the vibrating surface rotates the polarization of both pulses by 90 degrees. The leading pulse therefore takes the longer path during the return trip, while the lagging pulse takes the shorter path. After emerging from the PBS pair, the two pulses overlap in time but are still orthogonally polarized with respect to each other. A

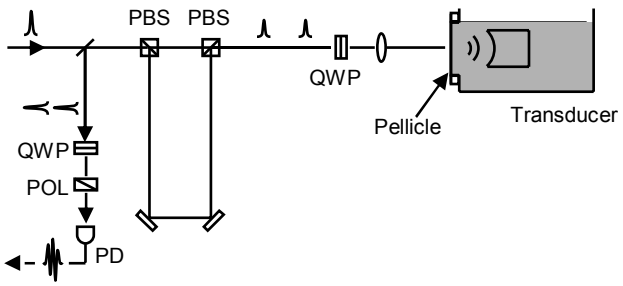

Figure 2. Detailed schematic of the Sagnac interferometer. Each polarizing beamsplitter (PBS) transmits horizontal polarization and reflects vertical polarization. The quarter wave plate (QWP) and pellicle rotate the polarization by 90 degrees. The return light is sent through a second QWP and polarizer (POL) before capture by the photodetector (PD).

QWP adds a π/2 phase bias between the two pulses, which is required for linear operation [5]. A polarizer oriented at 45 degrees mixes the two polarizations together before arriving at the amplified InGaAs photodetector.

B. Transducer characterization setup

The vibrating surface probed by the Sagnac interferometer is a 2.5 μm thick aluminized Mylar membrane [9]. This pellicle is positioned at the focus of a f/2 lithium niobate transducer [10] with a focal length of 3 mm. The focused optical spot size (i.e. $1/e^2$ diameter) on the pellicle is measured to be 8 μm. The optical power reaching the photodetector is approximately 0.9 mW. The detection bandwidth of the interferometer is 150 MHz, limited by the photodetector preamplifier. The transducer is laterally scanned over a 50 x 50 grid in 5 μm increments. The signal from each location is averaged 128 times by a 200 MHz 8-bit digital oscilloscope.

III. RESULTS

A. Time-domain

Fig. 3(a) shows the Sagnac signal at the peak of the transducer focus. The clean waveform suggests a high signal-to-noise ratio (SNR), which is limited by the digitizer. A single shot waveform was also acquired and computed to have a SNR of 23 dB. The Sagnac signal is similar to the pulse echo signal recorded from the transducer, as shown in Fig. 3(b).

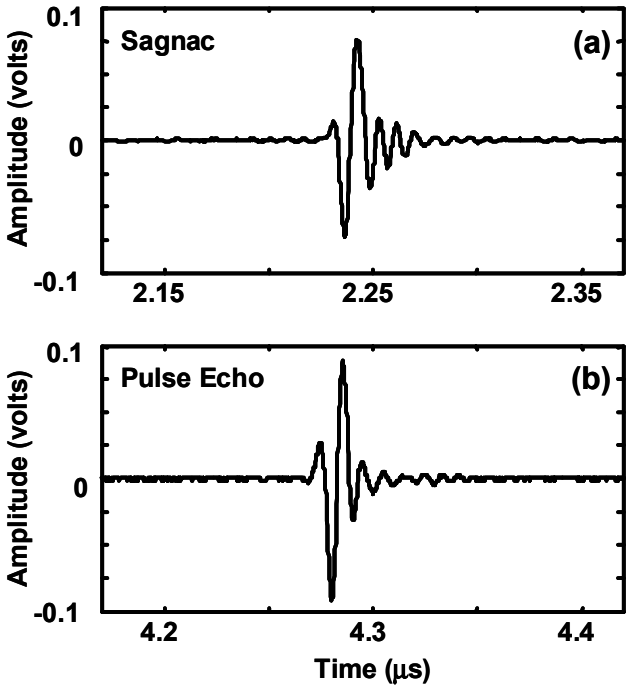

Figure 3. (a) Sagnac signal (128 averages) from the transducer focus. (b) Pulse echo signal (128 averages) recorded from the transducer. The tight pulses confirm the broadband output of the transducer.

B. Frequency domain

The Sagnac and pulse echo spectra are shown by the solid and dashed curves, respectively, in Fig. 4. The Sagnac spectrum has a peak frequency and -6 dB bandwidth of 80 MHz and 75 MHz, respectively. The pulse echo spectrum has corresponding values of 90 MHz and 70 MHz, respectively. The slight difference is expected since the pulse echo spectrum is shaped by the two-way response of the transducer. The Sagnac spectrum contains a null near 130 MHz, which is evident as the slight high frequency ringing on the tail end of the time-domain waveform in Fig. 3(a). This is attributed to an acoustic mode of the membrane, most likely the lowest order anti-symmetric A_0 or symmetric S_0 Lamb wave mode [11]. The exact mechanism is the subject of current investigation.

C. Spatial domain

A map of the peak intensity spanning 250 x 250 μm is shown over a 40 dB scale in Fig. 5. The Airy disk pattern of the transducer focus is clearly visible. Horizontal and vertical line-outs through the transducer focus reveal a -3 dB transmit beam width of 40 μm along both axes and a sidelobe level of -21 dB. The 8 μm spot size of the Sagnac interferometer's optical beam can clearly sample the spatial profile of the high frequency transducer focus.

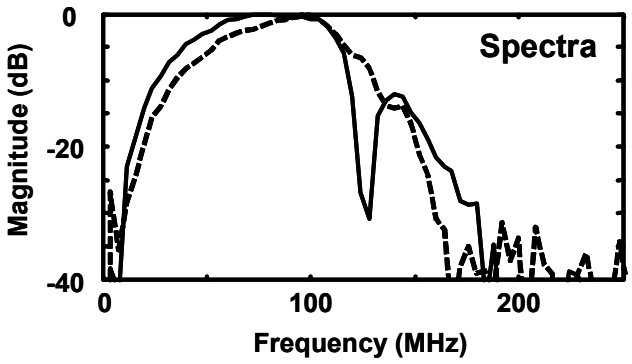

Figure 4. Spectra of the Sagnac signal (solid curve) and pulse echo signal (dashed curve). The frequency null at 130 MHz indicates the excitation of a membrane mode.

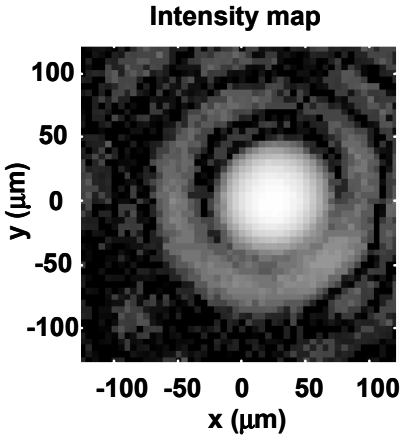

Figure 5. Map of peak ultrasound intensity shown over a 40 dB scale. The scanned region covers a 250 x 250 μm area.

D. Calibration

The Sagnac interferometer is calibrated at lower frequencies by comparison to a PVDF hydrophone with an active element diameter of 85 μm [12]. The ultrasound source is a 25 MHz f/2 PZT transducer [13]. The Sagnac and PVDF hydrophone signals are shown in Fig. 6(a) and (b), respectively. The two waveforms are clearly very similar, suggesting a similar response over this frequency range. Based on the calibration data of the PVDF hydrophone, the Sagnac transfer function is computed to be 0.1 μV/Pa for frequencies less than 20 MHz.

The theoretical frequency response of the Sagnac interferometer is a sinc function, where the first zero is located at $f = 1/\tau = 500$ MHz. Therefore, the 0.1 μV/Pa response represents the maximum response of the interferometer. This sinc-shaped transfer function must be deconvolved from the Sagnac voltage signal to yield a pressure signal. Performing this deconvolution in the frequency domain is complicated by the zeros of the sinc function. The sinc function is approximated as a Gaussian function to simplify the spectral inversion. However, this crude approximation produces a decent fit for frequencies less than 250 MHz, which is more than sufficient bandwidth for this experiment. Dividing the spectrum of the Sagnac voltage signal by this Gaussian transfer function leads to the pressure waveform. A maximum pressure of approximately 0.75 MPa, as shown in Fig. 7, is measured from the high frequency lithium niobate transducer.

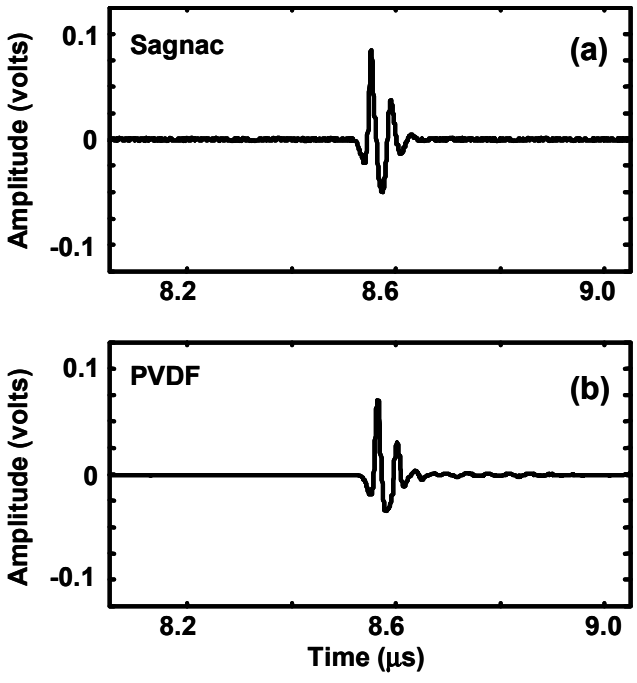

Figure 6. 25 MHz transducer measurement taken with the (a) Sagnac interferometer (b) calibrated PVDF hydrophone.

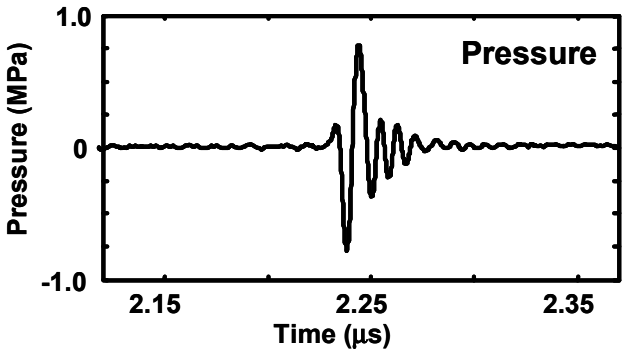

Figure 7. Pressure waveform obtained from the Sagnac measurement of the high frequency lithium niobate transducer.

E. Sensitivity

The sensitivity of the Sagnac interferometer is determined by a single shot waveform, where the rms noise voltage is measured to be 3.8 mV. The Sagnac calibration leads to a noise equivalent pressure (NEP) of 38 kPa over an approximately 150 MHz bandwidth.

IV. DISCUSSION

The Sagnac interferometer clearly has sufficient spatial resolution, bandwidth, and sensitivity to characterize high frequency ultrasound transducers. However, the membrane mode at 130 MHz must be eliminated. A possible approach is to replace the membrane with a slab of polydimethylsiloxane (PDMS), which is a transparent silicone. The transducer focus is positioned on the PDMS surface in contact with water. A metallic coating can be deposited on this PDMS surface to reflect the Sagnac light. The advantage of this structure is the suppression of interface modes, due to excellent acoustic matching between PDMS and water. The PDMS must be sufficiently thick (e.g. 2 mm) to prevent reverberations from corrupting the acquired pressure waveform.

V. CONCLUSIONS AND FUTURE WORK

We have demonstrated high frequency transducer characterization with a Sagnac interferometer. The spatial resolution is 8 μm and bandwidth is over 150 MHz. The pressure-to-voltage conversion is approximately 0.1 μV/Pa. The single-shot noise equivalent pressure is 38 kPa. Signal averaging over 100 times can lower the NEP to less than 5 kPa, which is sufficient for most transducer measurements.

Future work includes developing a fiber optic version of the Sagnac interferometer, along with replacing the pellicle with a PDMS sensing surface. An immersible probe head will also be developed to simplify the operation of the Sagnac hydrophone.

ACKNOWLEDGMENT

Thousand thanks to (1) the Resource Center for Medical Ultrasonic Transducer Technology at the University of Southern California for fabricating the excellent lithium niobate transducer (2) NIH for research funding.

REFERENCES

[1] J.P. Monchalin, "Optical detection of ultrasound," IEEE Trans. Ultrason. Ferroelect. Freq. Contr., Vol. 33, 485-499 (1986).

[2] S. Ashkenazi, Y. Hou, T. Buma, and M. O'Donnell, "Optoacoustic imaging using thin polymer etalon," *Appl. Phys. Lett*., vol. 86, 134102 (2005).

[3] P.C. Beard, F. Perennes, and T.N. Mills, "Transduction mechanisms of the Fabry-Perot polymer film sensing concept for wideband ultrasound detection," *IEEE Trans. Ultrason. Ferroelect. Freq. Contr*., vol. 46, 1575-1582 (1999).

[4] V. Wilkens, C. Koch, and W. Moikenstruck, "Frequency response of a fiber-optic dielectric multilayer hydrophone", *Proc. IEEE Ultrason. Symp*., 1113-1116 (2000).

[5] J.J. Alcoz, C.E. Duffer, and S. Nair, "Noncontact detection of ultrasound with rugged fiber-optic interferometer," *Proc. IEEE Ultrason. Symp*., 639-642 (1996).

[6] P.A. Fomitchov, S. Krishnaswamy, J.D. Achenbach, "Compact phase-shifted Sagnac interferometer for ultrasound detection," *Opt. Laser Technol*., vol. 29, 333-338 (1997).

[7] T.S. Jang, S.S. Lee, I.B. Kwon, W.J. Lee, and J.J. Lee, "Noncontact detection of ultrasonic waves using fiber optic Sagnac interferometer," *IEEE Trans. Ultrason. Ferroelect. Freq. Contr*., vol. 49, 767-774 (2002).

[8] K. Takada, "Noise in optical low-coherence reflectometry," *IEEE J. Quantum Electron*., vol. 34, 1098-1108 (1998).

[9] National Photocolor, Inc., Mamaroneck, NY.

[10] Resource Center for Medical Ultrasonic Transducer Technology, University of Southern California, Los Angeles, CA.

[11] D.A. Hutchins, K. Lundgren, and S. B. Palmer, "A laser study of transient Lamb waves in thin materials," J. Acoust. Soc. Am., Vol. 85, 1441-1448 (1989).

[12] Onda Corp., Sunnyvale, CA.

[13] Olympus NDT, Waltham, MA.